Journal of Membrane Science 378 (2011) 280–289

Contents lists available at ScienceDirect

Journal of Membrane Science

journal homepage: www.elsevier.com/locate/memsci

Ultrafiltration of supercoiled plasmid DNA: Modeling and application

António M. Morão[a,*], José C. Nunes[a], Fani Sousa[a], Maria Teresa Pessoa de Amorim[b], Isabel C. Escobar[c], João A. Queiroz[a]

[a] Centro de Investigação em Ciências da Saúde, University of Beira Interior, 6201-001 Covilhã, Portugal
[b] Department of Textile Engineering, University of Minho, 4800-058 Guimarães, Portugal
[c] Department of Chemical and Environmental Engineering, University of Toledo, Toledo, OH 43606, United States

ARTICLE INFO

Article history:
Received 11 March 2011
Received in revised form 8 May 2011
Accepted 9 May 2011
Available online 17 May 2011

Keywords:
Ultrafiltration
Plasmid DNA
Monte Carlo simulations
Sieving coefficients
Modeling

ABSTRACT

A mass transfer model is proposed for predicting sieving coefficients, S_{obs}, of supercoiled plasmid DNA (pDNA), in the presence of a salt, in membranes with narrow pores, *i.e.*, pores smaller than the gyration radii of the plasmids to be considered for a certain application. The model assumes that permeation occurs due to plasmid suction at the membrane surface as a result of the convective flow, being the probability of permeation also dependent on the instantaneous molecular conformation of the plasmid, when getting close to the pore. Two different approaches are tested to model plasmid structure, that of a closed segmented chains (CSC) of double stranded DNA, and that of considering the superhelical chain as a freely jointed chains (FJC). Both approaches were used to estimate the radius of gyration, r_g, of different plasmids by statistical simulation, and the obtained values were compared with experimental data available in the literature.

A 6050 bp plasmid, *pVAX1-LacZ*, was used in the experimental work, in which filtration tests were performed using three different ultrafiltration membranes of known pore size, in a 10 ml stirred cell. At constant ionic strength, sieving coefficients were determined as a function of the permeate flux, J_v, at two different values of stirring speed, ω. The results are in very good agreement with the model predictions at the highest stirring speed and the observed deviations found at the lowest stirring speed were interpreted with the aid of the developed model by considering the possibility of plasmid adsorption. Then, it was investigated the effect of changing the ionic strength of the medium at constant J_v and ω. The obtained results clearly agree with the model predictions.

1. Introduction

The application of membrane separation techniques for plasmid DNA (pDNA) purification has been investigated in recent years, aiming at its production in large scale, for applications in gene therapy and DNA vaccines [1–8]. Plasmids are conventionally produced by fermentation, which is followed by cell lysis and further purification steps, usually involving precipitation steps with salts and solvents and at least one chromatographic step, which is generally required to obtain a product of adequate purity. Membranes have a great potential to be used in the downstream process of pDNA production, namely for solid–liquid separations, concentration/buffer exchange and sterilization [9–15]. Facing this possibility of different applications, it is of general interest to know the ability of these molecules to permeate through porous matrices, in order to choose *a priori* the adequate membranes for each application.

In terms of molecular geometry, plasmids are long and flexible circular molecules, capable of adopting supercoiled structures, depending on the properties of the medium. Being long and flexible, plasmids have very different sieving characteristics from rigid molecules whose transmission through membrane pores can be approached to that of hard spheres. Therefore, models such as those developed by Deen et al. [16], Bowen et al. [17], Noordman and Wesseling [18] and further developed by Morão et al. [19] are not applicable to plasmids. In fact, the possibility of deformation/elongation enables plasmids to permeate through pores of significantly lower size than their molecular hydrodynamic radii as reported by several previous studies [14,15,20–24]. With theoretical models available in literature [21–23,25], it is possible to estimate the critical flux above which the elongation of plasmids is high enough to enable permeation.

Permeation of plasmids through membranes also depends on the ionic strength of the media [22,26]. Typically it was

* Corresponding author. Tel.: +351 275 329 002; fax: +351 275 329 099.
E-mail address: ammorao@ubi.pt (A.M. Morão).

0376-7388/$ – see front matter © 2011 Elsevier B.V. All rights reserved.
doi:10.1016/j.memsci.2011.05.017

Nomenclature

a	persistence length (m)
a_s	parameter in Eq. (10) (m)
a^*	persistence length of uncharged DNA (m)
b	spacing between DNA charge sites (m)
c	concentration of the solute inside the pore (mol m^{-3})
C_b	concentration of the solute in the bulk of the solution being filtered (mol m^{-3})
C_m	concentration of the solute in the solution near the membrane in the absence of adsorption (mol m^{-3})
C_M	concentration of the species in the film of adsorbed plasmid near the membrane (mol m^{-3})
C_p	concentration of the solute in the permeate (mol m^{-3})
D_∞	diffusion coefficient (m^2 s^{-1})
$\langle h^2\rangle^{1/2}$	average end-to-end distance of a polymer chain (m)
I	ionic strength (mol m^{-3})
J_v	volumetric flux though the membrane (m s^{-1})
k	mass transfer coefficient (m s^{-1})
l_B	Bjerrum length for pure water (m)
l_k	length of the segments in a polymer chain (m)
l_K	Kuhn distance (m)
L	contour length of a polymer chain (m)
L_s	parameter in Eq. (10) (m)
nbp	number of base pairs
N	number of atoms in a molecule
N_A	Avogadro number (mol^{-1})
n_k	number of segments in a polymer chain
Q_x	surface charge in the adsorbed plasmid layer (mol m^{-3})
R	gas constant (J mol^{-1} K^{-1})
R_{DNA}	radius of DNA double-helix (m)
r_{cell}	cell radius (m)
r (i = 0, 1,. . ., $N-1$)	distance of a theoretical dot mass from the mass centre of a polymer chain in the FJC and CSC models (m)
r_g	average gyration radius (m)
r_g^*	instantaneous radius of gyration (m)
r_p	pore radius (m)
r_s	average hydrodynamic radius (m)
S_m	intrinsic sieving coefficient
S_{obs}	observed sieving coefficient
T	absolute temperature (K)
z	electric charge of an ion; in Eq. (8) is the cation charge

Greek symbols

α	parameter in Eq. (9)
δ	concentration polarization layer thickness (m)
ε	membrane porosity
Φ	dynamic steric partition coefficient
η	viscosity (Pa s)
κ	inverse Debye length (m^{-1})
λ_g	the ratio of $\langle h^2\rangle^{1/2}$ to the gyration radius
λ_h	the ratio of $\langle h^2\rangle^{1/2}$ to the pore radius
λ_s	the ratio of $\langle h^2\rangle^{1/2}$ to the hydrodynamic radius
θ	fractional coverage of the surface
ρ	density (kg m^{-3})
ω	angular velocity (rad/s)
ξ	DNA charge density
Ψ	electric potential (V)

observed in these studies an increase in permeation as the ionic strength increases, up to 150–200 mM, even in the case of permeation through non-charged membranes. This phenomenon was attributed to conformational changes of the plasmids with the decrease of electrostatic repulsion between their phosphate groups, as the ionic strength increases, thus becoming more compact molecules [22].

Following an independent approach for explaining the permeation of long flexible molecules through membranes with narrow pores, Morão et al. [27] developed a model for the estimation of the solute partition coefficient at the membrane surface, Φ, under the assumption that, besides molecular deformation induced by the flow, it is also required for permeation that the molecule has an adequate molecular conformation and orientation, when approaching the pore. For that purpose, a Monte Carlo method was developed to estimate the probability of permeation under dynamic conditions of filtration, which can be identified with Φ [27]. For obtaining the values of Φ, the molecules were modeled as freely jointed chains (FJC) and the authors found a relationship between Φ and λ_h (Eq. (14) of [27]) where λ_h is the ratio between the root mean square of the end-to-end distance of the polymer chain to the pore radius, $\langle h^{1/2}\rangle^2/r_p$. Alternatively, one can calculate Φ as a function of λ_g where λ_g is the ratio between the average radius of gyration to the pore radius, r_g/r_p. The applicability of that model was previously tested with two linear polymers: a dextran and a linear double stranded DNA molecule. The latter was obtained from a supercoiled plasmid by cutting the circular double stranded DNA chain with a restriction enzyme [27].

The present study aims at obtaining a model for prediction of plasmid DNA transmission, in its intact supercoiled isoform. Two basic models for representing the structure of these molecules are discussed here, that of closed segmented chains (CSC) and that of FJC. Moreover, it is shown here that Eq. (14) of [27], written in terms of λ_g can be used for obtaining Φ in the case of a CSC representation. From estimated values of Φ, observed sieving coefficients can be predicted using a mass transfer model developed here in which plasmids are modeled as polyelectrolytes. This model can be used also for the prediction of the ionic strength effect on plasmid permeation, by considering the addition of a salt.

2. Materials and methods

2.1. Set-up of the mass transfer model

To estimate the transmission of a plasmid through a membrane in the presence of a salt, a transport model with, at least, three ionic components has to be considered: the plasmid, denoted component "1", which is a polyanion of charge $-(2\ nbp)$ where nbp is the number of base pairs, due to the phosphate groups in its structure, an anion such as Cl^-, denoted component "2" and a cation such as Na^+, denoted component "3". The concentrations of 1 and 2 are typically known in the bulk of the solution to be filtered, $C_{b,1}$ and $C_{b,2}$, and if one considers that 3 is the counter ion of both components 1 and 2, its concentration will be given by a simple charge balance. A similar balance can be made at the solution near the membrane surface, if no adsorption occurs, where the concentrations of the species are $C_{m,i}$. These are different from $C_{b,i}$ due to the occurrence of concentration polarization.

At the membrane surface the solutes are distributed between the solution and the membrane pores according to their partition coefficients. Eq. (14) from [27] is used in all the calculations made here to estimate the steric partition coefficient of the plasmid,

Φ_1, with its parameters modified in order to obtain a relationship between Φ and λ_g:

$$\ln(\Phi) = a_0 + \frac{a_1}{2a_3}\left\{2a_4 \ln\left[\exp\left(\frac{x+a_3/2}{a_4}\right)+\exp\left(\frac{a_2}{a_4}\right)\right] - 2a_4 \ln\left[\exp\left(\frac{a_2+a_3/2}{a_4}\right)+\exp\left(\frac{x}{a_4}\right)\right]+a_3\right\} \quad (1)$$

$a_0 = -11.60$; $a_1 = 11.53$; $a_2 = 3.955$; $a_3 = -5.520$; $a_4 = -0.613$

$x = \ln(\lambda_g) + 0.896$; $\lambda_g = \frac{r_g}{r_p}$

All the membranes studied in this work were previously characterized in terms of pore radius, using the symmetric pore method (SPM) described in Morão et al. [19].

If one can neglect any charge effects on the partition process at the membrane surface, which can be a valid assumption if the membrane is uncharged, the partition coefficient of the plasmid corresponds to Φ_1.

Since the dominant mechanism of plasmid transport inside membrane with narrow pores is convection (diffusion should be negligible) and considering that, when permeating through membranes with $r_p < r_s$ plasmids should occupy the whole cross-section of the pores, under these particular conditions, Φ_1 can be identified with the intrinsic sieving coefficient $S_{m,1}$ [27]. By definition, the intrinsic sieving coefficients of the various components in the multicomponent system correspond to:

$$S_{m,i} = \frac{C_{p,i}}{C_{m,i}} \quad (2)$$

where $C_{p,i}$ are the concentrations in the permeate. The values of $S_{m,2}$ and $S_{m,3}$ are here approached to 1, assuming that the salts to be considered are not retained by the membrane; therefore $C_{p,i} = C_{m,i}$ for $i = 2$ and 3.

To complete the set-up of the mathematical model to be used for the calculations, a final set of relationships can be implicitly established between the concentrations $C_{p,i}$, $C_{m,i}$ and $C_{b,i}$ through the numeric integration of the extended Nernst–Planck (NP) equation across the concentration polarization layer [17]:

$$\frac{dC_{y,i}}{dy} = \frac{-z_i C_{y,i} F}{RT}\frac{d\Psi}{dy} + \frac{J_v}{D_i}(C_{y,i} - C_{p,i}) \quad (3)$$

where Ψ is the electric potential and $C_{y,i}$ are the concentrations at a distance $(\delta - y)$ from the membrane, being δ the thickness of the concentration polarization layer. The integration should be made under the condition of electroneutrality of the solution, which implies that:

$$\sum_{i=1}^{3} z_i \frac{dC_{y,i}}{dy} = 0 \quad (4)$$

A convenient algorithm for obtaining $C_{p,i}$ from $C_{b,i}$ and the membrane properties is proposed in Appendix I. From the estimated $C_{p,i}$ values one can calculate observed sieving coefficients, $S_{obs,i}$:

$$S_{obs,i} = \frac{C_{p,i}}{C_{b,i}} \quad (5)$$

which can be compared with experimental values obtained in filtration tests.

2.2. Estimation of the plasmid partition coefficient, Φ

For the application of the mass transfer model, previously defined, the partition coefficient of the plasmid has to be estimated, and for that purpose it is primarily necessary to define a structural model for representing this kind of molecules.

Being plasmids molecules of highly complex structure, it is desirable to consider a simplified way of representing their three-dimensional structure, when facing the problem of simulating their permeation through membranes. For that purpose two simplified approaches are discussed here, that of closed segment chains (CSC) and to consider plasmids as linear molecules.

2.2.1. Closed segmented chains (CSC) approach

The simplest model for representing circular polymers is that of closed segmented chains. A CSC representation of a certain circular macromolecule can be obtained by generating a FJC of the corresponding linear molecule with n_k segments of length l_k, as described in [27]; then, the first dot mass of the chain is moved to become at a distance l_k from the last dot mass, along the direction of the vector between the two points; then, the position of the second dot mass is adjusted by moving it to a distance l_k from the first dot mass in the same way, then the third, etc., and this process is repeated until all the distances between the dot masses are equal to l_k. By the use of such an iterative algorithm, three-dimensional representations of a circular molecule, with random conformations and random space orientations, are obtained. For each generated conformation the possibility of permeation through the membrane was tested using a similar procedure than that described in Morão et al. [27] for FJC. The process consists in aligning the mass centre of the molecule with the centre of the pore and also other 10 radial positions; it is tested then, for each radial position, if the closest dot mass of the molecule to the membrane surface is projected inside the pore, as condition for permeation to be allowed. By repeating these tests for a great number of times, typically above 10^5, one can obtain a radial distribution function of the probability of permeation of the molecule, and by integrating that function one obtains the total probability of permeation, which can be identified with the steric partition coefficient, Φ, of the solute between the solution near the membrane and inside the pores [28]. This partition coefficient should be viewed as a dynamic partition coefficient, since it can only be valid under dynamic conditions of filtration.

The radius of gyration of a certain molecule modeled as a CSC, can be directly determined, also, from the computational simulations of the molecular structure previously described. For that purpose, instantaneous radii of gyration, r_g^*, were determined each time the CSC was generated during the simulations, which is given by:

$$r_g^* = \sqrt{\frac{\sum_{i=0}^{N-1} r_i^2}{N}} \quad (6)$$

in the case of a chain made by equal dot masses [27]. Then, after 10^5 repeated simulations, at least, the average value, r_g, was calculated.

Values of Φ for CSC are represented in Fig. 1a as a function of n_k for different values of L/r_p, where L is the contour length of the chain and r_p the pore radius; the obtained values are compared with those of FJC, obtained previously by Morão et al. [27]. As it can be seen, Φ values for CSC are slightly higher than those of the corresponding FJC, especially when the number of segments of the chain is low. However, the dynamic partition coefficient dependency on r_g is the same for both CSC and FJC (see Fig. 1b). Thus, it can be concluded from these simulations that Eq. (1), which was obtained originally for FJC, is also valid for CSC.

From the simulations it was also obtained the following relationship that enables the estimation of r_g for a CSC as a function of n_k and L:

$$r_g = 0.221 n_k^{-0.352} L \quad (7)$$

For linear double stranded DNA the value of L can be estimated from the axial rising per each pair of bases, which is 0.34 nm [27] and the number of base pairs; this value should be similar for closed chains, *i.e.*, for pDNA. In order to estimate the value of n_k it is necessary to know l_k; as a first approach one may consider that l_k is given by the Kuhn distance, l_K, of the corresponding linear molecule

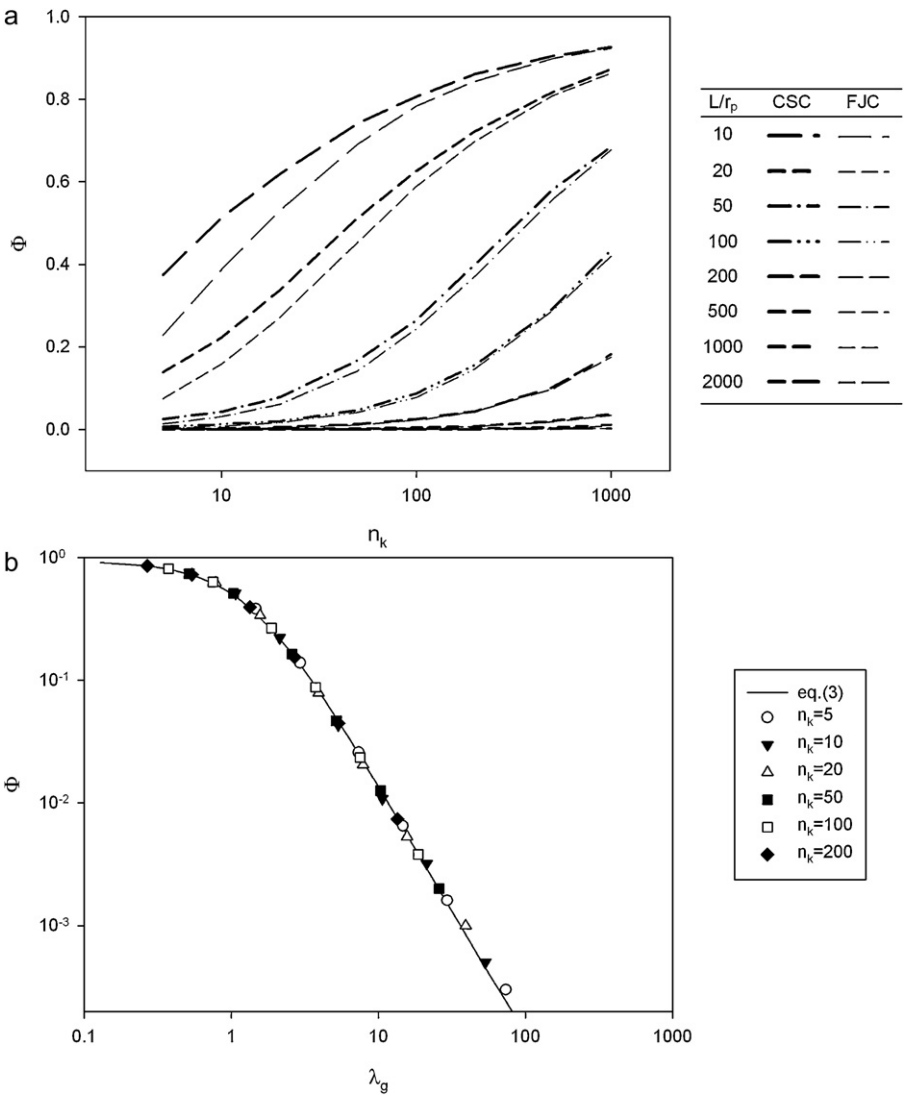

Fig. 1. Partition coefficient of circular segmented chains (CSC) and freely jointed chains (FJC) under filtration conditions: (a) as a function of n_k for various L/r_p and (b) as a function of the average ratio of λ_g.

(FJC). Values of the Kuhn distance for linear molecules correspond to approximately twice the value of the persistence length, a, which is a good approximation for $L/a > 10$ [27]. The persistence length of linear DNA is a function of the ionic strength of the solution, I, through the inverse Debye length, κ, and can be readily estimated from the following relationship [23,29]:

$$a = \left(\frac{\pi a^*}{2}\right)^{2/3} \frac{R_{DNA}{}^{4/3}}{z^2 l_B} \left[(2z\xi - 1)\frac{\kappa b e^{-\kappa b}}{1 - e^{-\kappa b}} - 1 - \ln(1 - e^{-\kappa b})\right] \quad (8)$$

However, l_k for a CSC is expected to be lower than l_K, taking into account that the molecular strain in a CSC should be higher than in a FJC. Considering, as a first approach, that the ratio of l_k to l_K is independent on the contour length, it is proposed here to introduce an empirical parameter, α, relating these two quantities:

$$l_k = \alpha l_K \quad (9)$$

An adequate method of obtaining α for circular DNA is from experimental values of r_g available in literature, using Eqs. (7)–(9). An optimum value of $\alpha = 0.196$ was found using a least squares method from data obtained for different plasmids at different ionic strength values (see Fig. 2). With this knowledge, the estimation of l_k from l_K becomes possible for any other plasmid using Eq. (9). To check for the accuracy of such predictions, one can use recently obtained radii of gyration of 5.76, 9.80 and 16.8 kbp plasmids, determined by static light scattering that were found to be 102 ± 2, 117 ± 3 and 169 ± 4 nm, respectively, at a constant ionic strength of 230 mM [30]; from the previous analysis it is possible to predict, for these three plasmids the values of 86, 121 and 171 nm, respectively, which can be considered a good approach.

2.2.2. Freely jointed chains (FJC) approach

Although not linear molecules, plasmids can also be modeled as FJC, but only under conditions of high ionic strength. In fact, when highly supercoiled, plasmids geometrically behave as long linear molecules, as it can be seen in AFM images obtained at high ionic strength (160 mM) [32].

Under this approach Eq. (1) can be used with r_g values calculated from the worm-like chain model, WLC, using the following expression [27,21–23]:

$$r_g = a_s \left[\frac{L_s}{3a_s} - 1 + \frac{2a_s}{L_s} - 2\left(\frac{a_s}{L_s}\right)^2 (1 - e^{-L_s/a_s})\right]^{1/2} \quad (10)$$

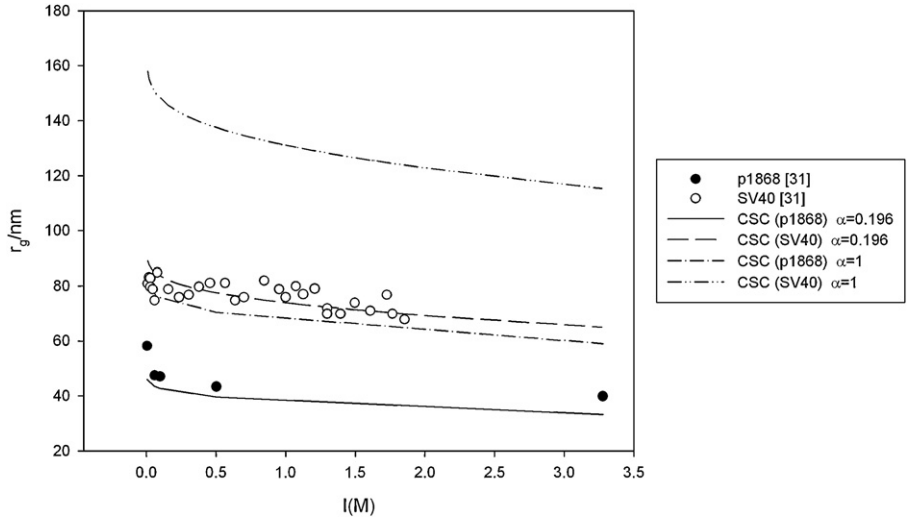

Fig. 2. Radii of gyration for plasmids p1868 (1868 bp) and simian virus 40, SV40 (5243 bp) as a function of the ionic strength [31]. Adjusted trend lines using Eqs. (7)–(9) with $\alpha = 0.196$ and $\alpha = 1$.

The subscript "*s*" used here indicates "superhelix", to note that on application of Eq. (10) to pDNA the values of the persistence length, a_s, and the contour length, L_s, refer to the superhelix and not to the dsDNA chain.

Values of L_s and a_s are not known *a priori*, however L_s as a first approach can be estimated as $0.5L$, where L is the contour length of the dsDNA chain (*i.e.*, L is given by 0.34 nm multiplied by the number of base pairs and the L_s value for a certain pDNA molecule corresponds to its maximum possible extension) and then one can adjust a_s from known values of r_g, using Eq. (10). A different approach was proposed by Latulippe et al. [30] by considering for plasmids an effective contour length of $0.4L$, when $a_s = 46$ nm, which is in a better agreement with the value of $L_s/L = 0.41$ previously reported by Boles et al. [33].

2.2.3. Comparison of the two approaches

The CSC and FJC approaches to model supercoiled pDNA under conditions of ionic strength higher than 0.2 M are compared in Fig. 3. As it can be seen, the best approach is clearly that of CSC,

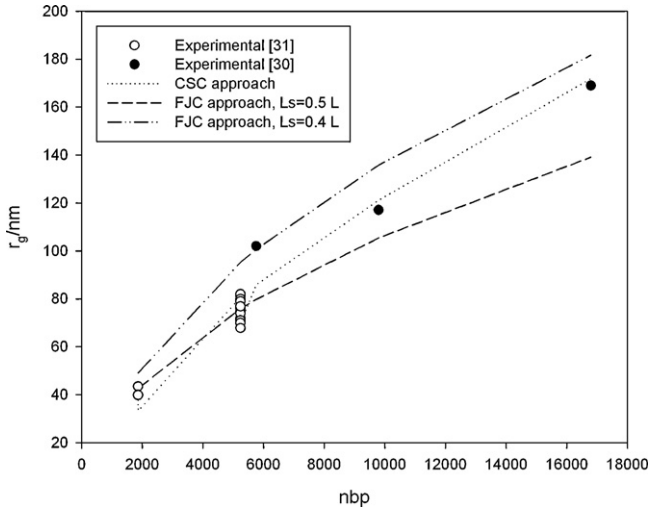

Fig. 3. Comparison of different approaches for the estimation of plasmid gyration radii. The following values of a_s were used in the case of the FJC model: 20.8 nm (adjusted value) in the case of considering $L_s = 0.5L$ and 46 nm from [31] in the case of considering $L_s = 0.5L$. Experimental gyration radii are from Latulippe et al. [30] and Hammermann et al. [31].

which gives an average error on the calculated r_g less than 4%. Therefore, this was the model selected for the calculations.

Using this approach one can estimate the dynamic partition coefficient of plasmids as function of their number of base pairs and the pore radius of the membrane (see Fig. 4).

2.3. Experimental detail

A 6050 bp plasmid, *pVAX1-LacZ*, was used in the experimental work reported here. The plasmid was produced by a cell culture of *E. coli* DH5α, then isolated and purified as described in Sousa et al. [34], with the purity of the final product being checked by agarose gel electrophoresis. All plasmid solutions used in the tests were prepared in a buffer solution consisting of 10 mM Tris/HCl at pH = 8.0 with addition of 0.45 M NaCl, except in tests where the effect of the ionic strength on the sieving coefficients was investigated. In those tests, appropriate amounts of NaCl were added to the same buffer solution to obtain different values of ionic strength.

The membranes used and their main characteristics are indicated in Table 1. As it can be seen, all the membranes have similar pore radii but different membrane materials; in the case of the track-etched polycarbonate (TEPC) membrane the pore size distribution is known from Kim et al. [35]; for both XM300 and YM100 membranes average pore radii were determined from rejection data of neutral solutes, using the symmetric pore model (SPM) described in Morão et al. [19]; the obtained values of r_p are indicated in Table 1.

Filtration tests were performed in a 10 ml stirred cell from *Amicon*/*Millipore*, model *8010*, with an effective filtration area of 4.1×10^{-4} m^2. Before filtration of the plasmid solutions the membranes were kept in water overnight in the dark and then flushed in the cell with 20 ml of the buffer solution to ensure the complete removal of possible contaminants, namely preservatives in the new membranes to be used. The buffer solution was then removed from the filtration cell and replaced by 10 ml of plasmid solution to be filtered. A sample of the feed solution was collected immediately before filtration. The stirring speed, ω, was set at 100 and 800 min^{-1} (previous calibration was performed) and the temperature in all the tests was 20 ± 1 °C. The permeate flow was controlled in all tests, using a *Watson-Marlow 403 U* peristaltic pump, placed after the membrane (thus imposing the permeate flux by suction); this pump has 10 rotating cylinders, and this ensures an almost non-pulsed flow. Before collecting the permeate samples to be analyzed, the first 1.0 ml of filtrate was collected in a Eppendorf tube to be

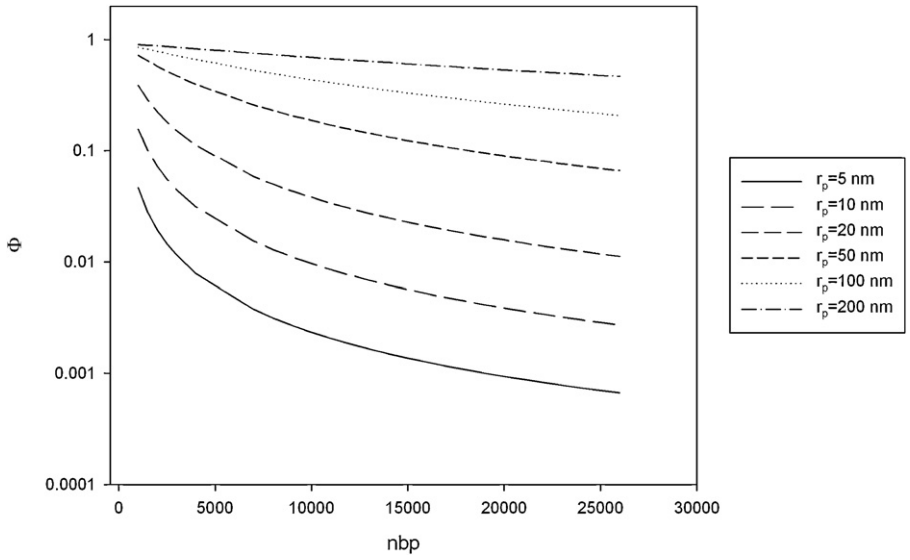

Fig. 4. Dynamic partition coefficient of plasmids as a function of the number of base pairs in membranes with different pore size.

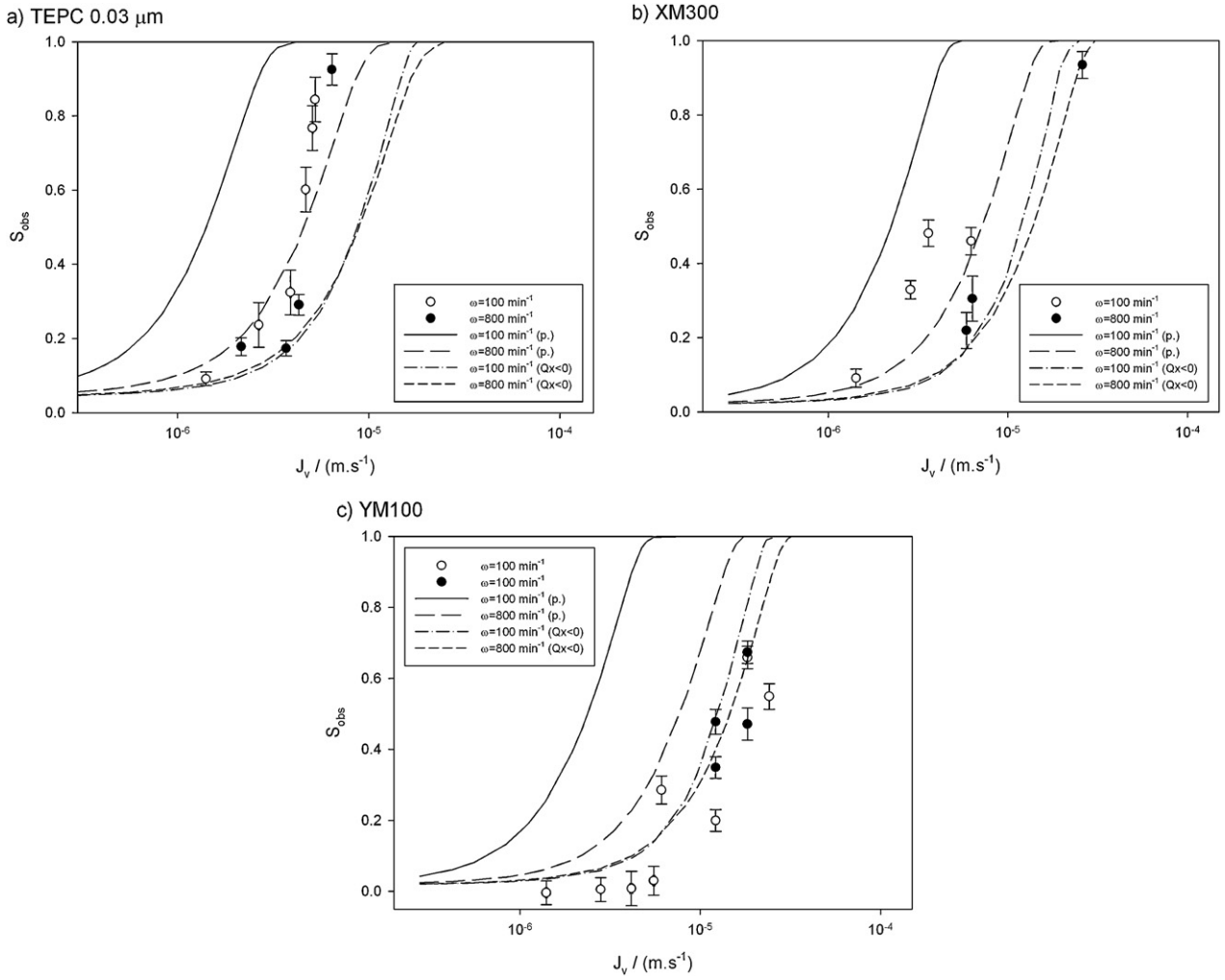

Fig. 5. Observed and predicted (p.) sieving coefficients of plasmid *pVAX1-LacZ* on membrane TEPC 0.03 μm as a function of the permeate flux for different values of stirring speed. Corrected curves by considering negative charge on the membrane surface due to adsorption ($Q_x < 0$).

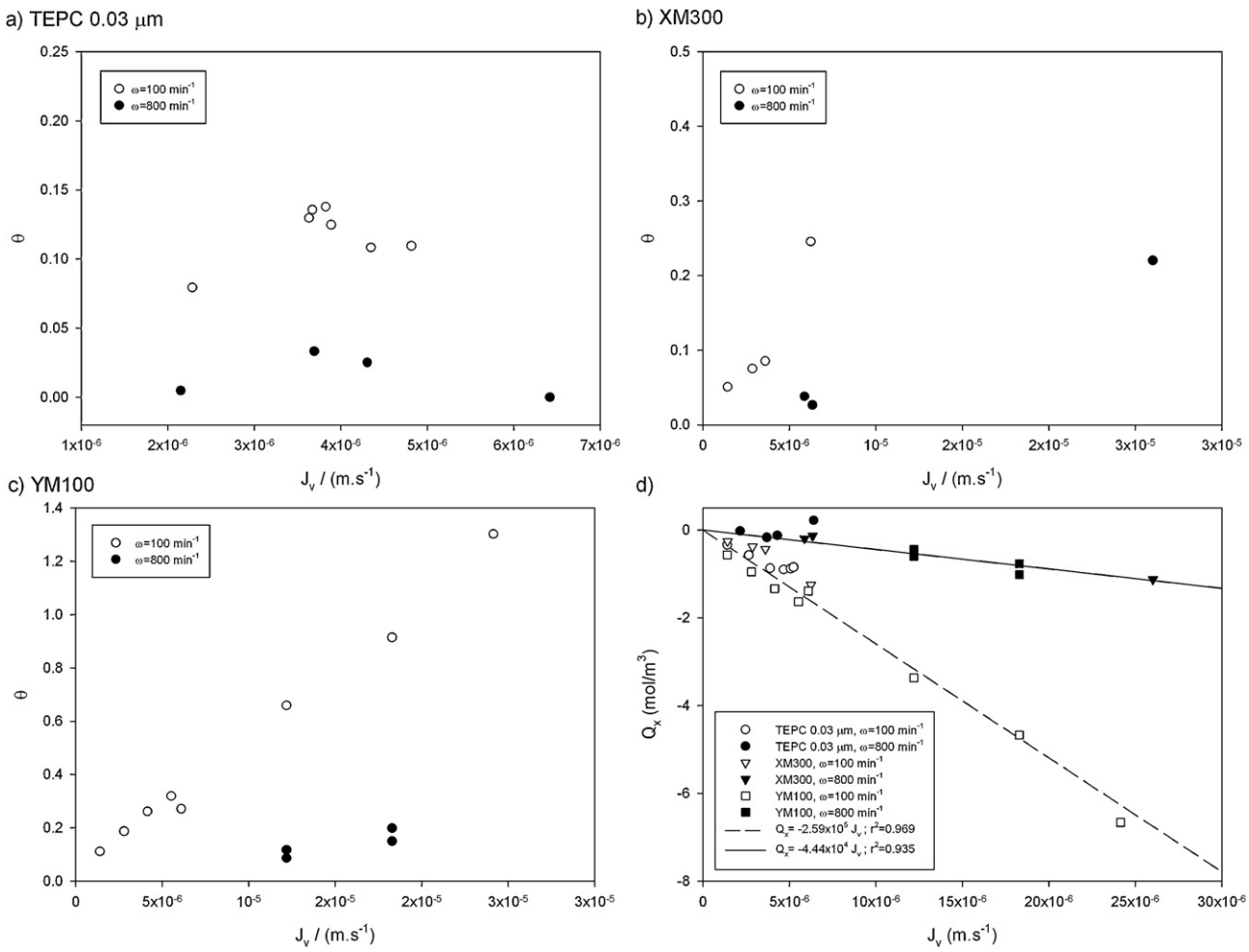

Fig. 6. Fractional coverage of the membrane surface by plasmid adsorbed molecules, θ, and total charge of the adsorbed molecules, as a function of the permeate flux, for the two stirring speed values tested. Values obtained from the data shown in Fig. 5.

rejected. This procedure avoided any significant dilution of the permeate samples by the buffer solution initially present in the tubes of the peristaltic pump, as experimentally checked. The permeate volume collected for each sample was 0.6 ml (thus a total permeate volume of 1.6 ml was collected). Plasmid concentrations, in both permeates and feed solutions, were determined by measuring the absorbance at 260 nm, with a *Ultrospect 3000* spectrophotometer from *Pharmacia Biotech*.

3. Results and discussion

Using the CSC approach, the gyration radius of plasmid *pVAX1-LacZ* was estimated to be 85.6 nm at the ionic strength of 0.46 M, which is approximately the value used in all the tests (except those were the ionic strength was varied). From this value and the pore radii values given in Table 1, the dynamic partition coefficients of the plasmid on the various membranes can be readily estimated using Eq. (1). The obtained values are indicated in Table 2. Using these values, observed sieving coefficients were estimated by numerically solving the set of Eqs. (1)–(5), with δ being estimated as:

$$\delta \simeq \frac{D_1}{k_1} \tag{11}$$

where k_1 is the mass transfer coefficient of the plasmid obtained from the following well-established correlation valid for stirred cells [36,37]:

$$\frac{kr_{cell}}{D_\infty} = 0.23\left(\frac{\omega r_{cell}^2 \rho}{\eta}\right)^{0.567}\left(\frac{\eta}{\rho D_\infty}\right)^{0.33} \tag{12}$$

Table 1
Main characteristics of the membranes used.

Membrane	Material	Supplier	r_p (nm)	ε	L (μm)
TEPC 0.03 μm	"track etched" polycarbonate	Sterlitech, USA	15[a]; 14.5[b]	4.2×10^{-3} [c]	6[c]
XM300	Polyacrylonitrile	Millipore	10.5[d]	–	–
YM100	Regenerated cellulose	Millipore	10.0[e]	–	–
Nylon 0.2 μm	Nylon	Millipore	100[a]	–	–

[a] Nominal value.
[b] Calculated from the pore size distribution.
[c] From the supplier.
[d] From Morão et al. [27].
[e] Experimentally determined using Dextran T70 and Ficoll 70 as reference solutes by the method described in [19].

The diffusion coefficient of plasmid *pVAX1-LacZ* was estimated to be 2.97×10^{-12} m^2 s^{-1}, using the correlation proposed by Prazeres et al. [38].

The observed sieving coefficients of plasmid *pVAX1-LacZ* on membranes TEPC 0.03 μm, XM300 and YM100, for different stirring speeds, as a function of the flux are shown in Fig. 5 and compared with the corresponding theoretical predictions.

As it can be seen in Fig. 5, the pure theoretical predictions (p.) based on the proposed model agree with the observation that intermediate sieving coefficients of the plasmid are found in the range of permeate flux values tested and at the highest stirring speed clearly approach the experimental results.

The observed sieving coefficients are, however, generally lower than predicted; this suggests the occurrence of an excessive accumulation of the plasmid at the membrane surface or fouling, which should be more intense at the lowest stirring speed.

To further analyze these possible plasmid/surface interactions, one can consider the hypothesis that plasmid adsorption occurs at the membrane surface. In that case the surface would become negatively charged due to the fact that plasmids are highly negatively charged molecules, and this could possibly explain the observed deviations between the observed and predicted values. To investigate for this possibility, the algorithm previously described for the estimation of S_{obs} can be modified in order to allow an estimate of the surface charge, Q_x, from the experimental values of S_{obs}. Then, from the obtained Q_x values the fractional coverage of the surface, θ can be estimated. Details of the algorithm used in these calculations are indicated in Appendix II. The obtained values of Q_x and θ, are shown in Fig. 6, as a function of the permeate flux. As it can be seen, very reasonable values of θ are obtained, on the basis that a monolayer of adsorbed plasmid molecules is formed at the surface of the membranes. For each membrane, the fractional coverage is clearly higher at the lowest stirring speed and for the *YM100* membrane the highest values of θ are obtained, which reflects the higher deviations of S_{obs} from the theoretical predictions, found for this membrane. About the values of Q_x it is found a linear dependency of Q_x on J_v and that dependency is apparently independent of the membrane used. With the aid of the correlations indicated in Fig. 6d, a better model description of the dependency of S_{obs} on J_v and ω can be made, by considering the effect of surface charge on S_{obs}, instead of assuming $Q_x = 0$, in the calculations (see Fig. 5).

Apart from the effects of pore size, flux and stirring speed in plasmid S_{obs} it is also important to understand the effect of the ionic strength, which markedly affects it. Observed sieving coefficients of the plasmid, obtained at different values of ionic strength in the TEPC 0.03 μm membrane and also in a 0.2 μm nylon membrane, are shown in Fig. 7, and can be compared with model predictions assuming negligible adsorption, *i.e.*, $Q_x = 0$. As it can be seen, at high values of ionic strength the sieving coefficients are very high and as the ionic strength decreases, a sharp transition is observed near 50 mM in the case of the TEPC 0.03 μm membrane, towards very low values of S_{obs}, as predicted by the model. In the case of the 0.2 μm membrane, which has larger pores, the ionic strength transition value is apparently lower, near 10 mM, as predicted by the model, also. The dominant factor that leads to the observed

Table 2
Dynamic partition coefficients of plasmid *pVAX1-LacZ* on the membranes studied at the ionic strength of 0.46 M.

Membrane	Φ
TEPC 0.03 μm	0.0409[a]; 0.0418[b]
XM300	0.0205
YM100	0.0187
Nylon 0.2 μm	0.57

[a] Using the nominal value of pore size.
[b] Using the pore size distribution.

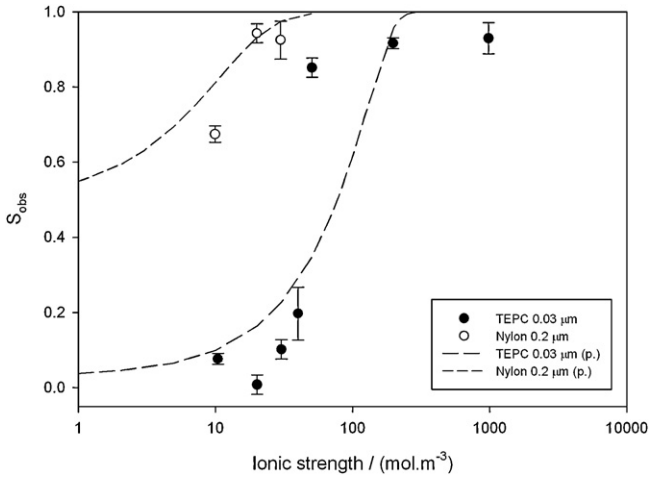

Fig. 7. Observed and predicted (p.) sieving coefficients of plasmid *pVAX1-LacZ* on membranes TEPC 0.03 μm at $J_v = 5.0 \times 10^{-6}$ m s^{-1} and Nylon 0.02 μm at $J_v = 4.2 \times 10^{-6}$ m s^{-1}, as a function of the ionic strength of the medium. $\omega = 100$ min^{-1}.

decrease in S_{obs} is the decrease of plasmid concentration near the membrane surface, *i.e.*, the $C_{m,1}$ values (see Fig. 8). This is a consequence of the higher repulsion that occurs between plasmid molecules at the membrane surface as the salt concentration is

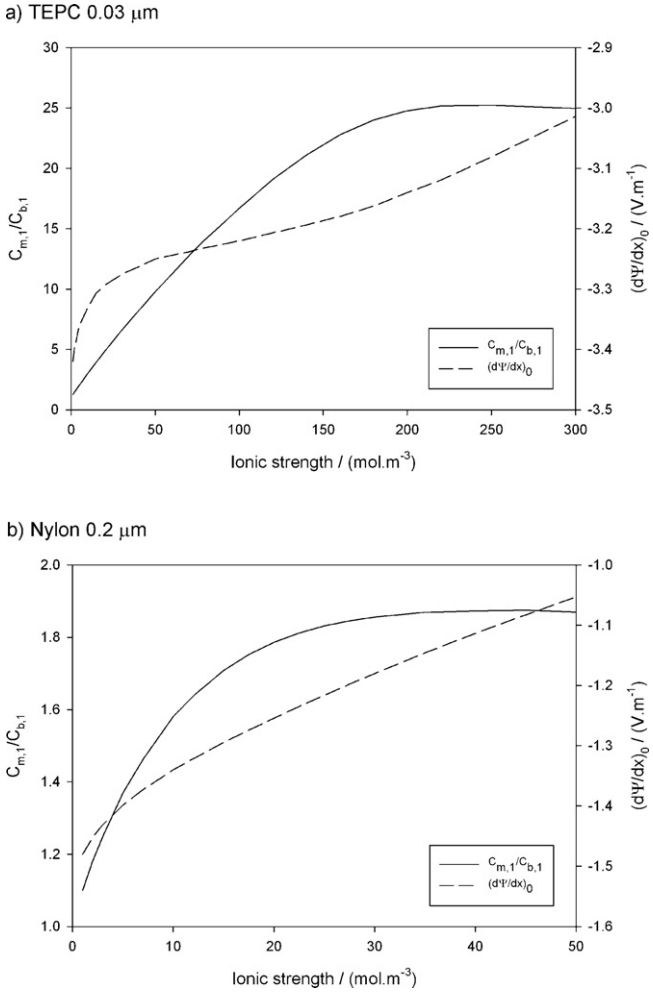

Fig. 8. Concentration of the plasmid at the membrane surface to plasmid bulk concentration ratio, $C_{m,1}/C_{b,1}$, and electric potential gradient at the membrane surface, as predicted by the model, assuming negligible adsorption, *i.e.*, $Q_x = 0$.

decreased, which can be inferred from the increase, in absolute value, of the electric potential gradient near the membrane surface, $(d\Psi/dx)_0$, as the ionic strength decreases (see also Fig. 8).

4. Conclusions

A mass transfer model was developed for predicting the sieving coefficients of plasmids in membranes with narrow pores. Under these circumstances it is considered that permeation only occurs due the suction effect of the convective flow and plasmids occupy the whole cross-section of the pore while permeating, being convection the only transport mechanism inside the pore. At the membrane surface plasmid molecules tend to accumulate due to concentration polarization; however this accumulation is counterbalanced by the intermolecular electric repulsion of the plasmid molecules, that are highly negatively charged.

The accuracy of the predictions of the developed model was found to be significantly dependent on the hydrodynamic conditions used, more specifically the stirring speed and also the imposed permeate flux. However, the observed deviations between the experimental results and the predictions can be interpreted with the aid of the developed model, by considering that adsorption of plasmid molecules occurs under conditions of excessive accumulation at the membrane surface. In that case, it is proposed that a monolayer of plasmid molecules is formed, which imparts negative charge to the membrane surface. In that case, plasmid molecules would be partially excluded from the region near the pores, which leads to the observed decrease of the sieving coefficients in respect to the model predictions.

Apart from the hydrodynamic effects, the accumulation of plasmid molecules at the membrane surface can be counterbalanced also by decreasing the ionic strength of the medium, since plasmid molecules are highly negatively charged and therefore the intermolecular electric repulsion is enhanced. Very accurate predictions of this effect are obtained with the model developed here.

Acknowledgements

Fundação para a Ciência e a Tecnologia (FCT) for the financial support (PTDC/EBB-BIO/114320/2009) and the grants awarded to António M. Morão (SFRH/BPD27170/2006) and José C. Nunes (SFRH/BD/48801/2008).

Appendix I.

The first step of the proposed algorithm for the numeric calculation of $C_{p,i}$ is guessing the values of $C_{m,1}$ and $C_{m,2}$, then a value for $C_{m,3}$ is calculated. From these values, which will be denoted $C^0_{m,i}$ the concentrations in the permeate can be guessed: for the plasmid as $\Phi_1 C^0_{m,1}$ and for components 2 and 3 as $C^0_{m,2}$ and $C^0_{m,3}$ respectively, under the assumptions that convection is the only transport mechanism inside the pores, for the plasmid Φ_1 can be identified with the intrinsic sieving coefficient and that components 2 and 3 are not retained by the membrane. With these values of $C_{p,i}$ the differential equation set (3) with the conditions (4) can be solved, using the $C_{b,i}$ as initial conditions along a distance δ, which corresponds to the concentration polarization layer thickness (δ can be estimated from Eqs. (11) and (12)), thereby obtaining a new guess for the $C_{m,i}$ values, which will be denoted $C^1_{m,1}$; these can be compared with the previous guessed $C^0_{m,1}$. The following error function was used to compare the two sets of values:

$$f(C^0_{m,i}, C^1_{m,i}) = \sum_{i=1}^{3} \frac{|C^0_{m,i} - C^1_{m,i}|}{C_{b,i}} \tag{A1.1}$$

The absolute deviations are divided by the respective $C_{b,i}$ since the plasmid concentrations are always much smaller than those of the salt. In order to obtain the correct set of $C_{m,i}$ values, the initially guessed values of $C_{m,1}$ and $C_{m,2}$ can be varied along pre-established intervals, to find the minimum value of f.

Appendix II.

For these calculations an iterative method can be used in which an initial approach is made, $C_{p2} \approx C_{b2}$, and from the known values of C_{p1}, C_{p3} is then calculated. Then, from the values of C_{bi} and C_{pi}, Eq. (3) can be solved as previously described thereby obtaining the C_{mi} values. Considering that some plasmid molecules are adsorbed at the membrane surface, forming a negatively charged film, all the components in solution will be involved in a partition equilibrium, with the concentrations of non-adsorbed species in that film, $C_{M,i}$ being given by:

$$C_{M,i} = C_{m,i} \exp\left(\frac{z_i F}{RT}\Delta\Psi^*_{\mathrm{D}}\right) \tag{A2.1}$$

where $\Delta\Psi^*_D$ denotes the electric potential difference between the solution near the film and the film. Since $C_{M,1} = C_{p,1}/\Phi$, from the $C_{m,1}$ value the potential difference $\Delta\Psi^*_D$ can be calculated using Eq. (A2.1) in the form:

$$\Delta\Psi_{\mathrm{D}} = \frac{RT}{z_1 F}\ln\left(\frac{C_{M,1}}{C_{m,1}}\right) \tag{A2.2}$$

Then, the values of $C_{M,2}$ and $C_{M,3}$ can be calculated through Eq. (A2.1). With the $C_{M,2}$ value a new approach for C_{p2} is then obtained and the same calculations should be cyclically repeated, until convergence is obtained. Finally, with the obtained values of $C_{M,i}$, Q_x can be calculated from the charge balance at the adsorbed layer at membrane surface:

$$Q_x = -\sum_{i=1}^{3} z_i C_{M,i} \tag{A2.3}$$

Assuming that it is a monolayer of plasmid molecules that is formed at membrane surface, the fractional coverage of the surface can be estimated from the values of Q_x. First, it is calculated the number of adsorbed molecules, per unit of volume of the monolayer:

$$N_{ads} = -\frac{Q_x N_A}{2\,nbp} \tag{A2.4}$$

where N_A is the Avogadro number, taking into account that each pDNA molecule has (2 *nbp*) charged groups. By multiplying N_{ads} by a distance of twice the gyration radius of the plasmid, $2r_g$, it is obtained approximately the number of *pDNA* molecules adsorbed per unit of area. Since each plasmid molecule occupies an approximate area of πr_g^2, the fractional coverage of the surface will be given by:

$$\theta = -\frac{Q_x N_A}{nbp}\pi r_g^3 \tag{A2.5}$$

References

[1] D.F. Prazeres, T. Schluep, C. Cooney, Preparative purification of supercoiled plasmid DNA using anion-exchange chromatography, Journal of Chromatography A 806 (1998) 31–45.
[2] D.M.F. Prazeres, G.N.M. Ferreira, Design of flowsheets for the recovery and purification of plasmids for gene therapy and DNA vaccination, Chemical Engineering and Processing 43 (2004) 609–624.
[3] D.M.F. Prazeres, G.N.M. Ferreira, G.A. Monteiro, C.L. Cooney, J.M.S. Cabral, Large-scale production of pharmaceutical-grade plasmid DNA for gene therapy: problems and bottlenecks, Trends in Biotechnology 17 (1999) 169–174.
[4] A. Mountain, Gene therapy: the first decade, Trends in Biotechnology 18 (2000) 119–128.

[5] K.J. Prather, S. Sagar, J. Murphy, M. Chartrain, Industrial scale production of plasmid DNA for vaccine and gene therapy: plasmid design, production, and purification, Enzyme and Microbial Technology 33 (2003) 865–883.
[6] W.J. Kelly, Perspectives on plasmid-based gene therapy: challenges for the product and the process, Biotechnology and Applied Biochemistry 37 (2003) 219–223.
[7] J. Urthaler, C. Ascher, H. Wohrer, R. Necina, Automated alkaline lysis for industrial scale cGMP production of pharmaceutical grade plasmid-DNA, Journal of Biotechnology 128 (2007) 132–149.
[8] F. Sousa, D.M.F. Prazeres, J.A. Queiroz, Affinity chromatography approaches to overcome the challenges of purifying plasmid DNA, Trends in Biotechnology 26 (2008) 518–525.
[9] D.L. Varley, A.G. Hitchcock, A.M.E. Weiss, W.A. Horler, R. Cowell, L. Peddie, G.S. Sharpe, D.R. Thatcher, J.A.J. Hanak, Production of plasmid DNA for human gene therapy using modified alkaline cell lysis and expanded bed anion exchange chromatography, Bioseparation 8 (1999) 209–217.
[10] D.W. Kahn, M.D. Butler, D.L. Cohen, M. Gordon, J.W. Kahn, M.E. Winkler, Purification of plasmid DNA by tangential flow filtration, Biotechnology and Bioengineering 69 (2000) 101–106.
[11] A. Eon-Duval, R.H. Macduff, C.A. Fisher, M.J. Harris, C. Brook, Removal of RNA impurities by tangential flow filtration in an RNase-free plasmid DNA purification process, Analytical Biochemistry 316 (2003) 66–73.
[12] C. Kepka, R. Lemmens, J. Vasi, T. Nyhammar, P. Gustavsson, Integrated process for purification of plasmid DNA using aqueous two-phase systems combined with membrane filtration and lid-bead chromatography, Journal of Chromatography A 1057 (2004) 115–124.
[13] S.S. Freitas, M.L. Wu, G.A. Monteiro, D.M.F. Prazeres, J.A.L. Santos, Intermediate recovery of plasmid DNA using tangential flow filtration, in: Engineering with Membranes 2008, Vale do Lobo, Portugal, 2008.
[14] S. Kong, N. Titchener-Hooker, M.S. Levy, Plasmid DNA processing for gene therapy and vaccination: studies on the membrane sterilisation filtration step, Journal of Membrane Science 280 (2006) 824–831.
[15] S. Kong, J. Aucamp, N.J. Titchener-Hooker, Studies on membrane sterile filtration of plasmid DNA using an automated multiwell technique, Journal of Membrane Science 353 (2010) 144–150.
[16] W.M. Deen, Hindered transport of large molecules in liquid-filled pores, AIChE Journal 33 (1987) 1409–1425.
[17] W.R. Bowen, J.S. Welfoot, Modelling the performance of membrane nanofiltration—critical assessment and model development, Chemical Engineering Science 57 (2002) 1121–1137.
[18] T.R. Noordman, J.A. Wesselingh, Transport of large molecules through membranes with narrow pores: the Maxwell–Stefan description combined with hydrodynamic theory, Journal of Membrane Science 210 (2002) 227–243.
[19] A. Morão, M.T. Pessoa de Amorim, A. Lopes, I. Escobar, J.A. Queiroz, Characterisation of ultrafiltration and nanofiltration membranes from rejections of neutral reference solutes using a model of asymmetric pores, Journal of Membrane Science 319 (2008) 64–75.
[20] D. Kendall, G.J. Lye, M.S. Levy, Purification of plasmid DNA by an integrated operation comprising tangential flow filtration and nitrocellulose adsorption, Biotechnology and Bioengineering 79 (2002) 816–822.
[21] D.R. Latulippe, K. Ager, A.L. Zydney, Flux-dependent transmission of supercoiled plasmid DNA through ultrafiltration membranes, Journal of Membrane Science 294 (2007) 169–177.
[22] D.R. Latulippe, A.L. Zydney, Salt-induced changes in plasmid DNA transmission through ultrafiltration membranes, Biotechnology and Bioengineering 99 (2008) 390–398.
[23] D.R. Latulippe, A.L. Zydney, Elongational flow model for transmission of supercoiled plasmid DNA during membrane ultrafiltration, Journal of Membrane Science 329 (2009) 201–208.
[24] A.M. Morão, J.C. Nunes, F. Sousa, M.T. Pessoa de Amorim, I.C. Escobar, J.A. Queiroz, Modeling of supercoiled plasmid DNA transmission through an ultrafiltration membrane, in: International Congress on Membranes and Membrane Processes, ICOM 2008, Honolulu, Hawaii, 2008.
[25] S. Daoudi, F. Brochard, Flows of flexible polymer solutions in pores, Macromolecules 11 (1978) 751–758.
[26] K. Ager, D.R. Latulippe, A.L. Zydney, Plasmid DNA transmission through charged ultrafiltration membranes, Journal of Membrane Science 344 (2009) 123–128.
[27] A. Morão, J.C. Nunes, F. Sousa, M.T. Pessoa de Amorim, I.C. Escobar, J.A. Queiroz, Development of a model for membrane filtration of long and flexible macromolecules: application to predict dextran and linear DNA rejections in micro and ultrafiltration, Journal of Membrane Science 336 (2009) 61–70.
[28] M.G. Davidson, U.W. Suter, W.M. Deen, Equilibrium partitioning of flexible macromolecules between bulk solution and cylindrical pores, Macromolecules 20 (1987) 1141–1146.
[29] G.S. Manning, The persistence length of DNA is reached from the persistence length of its null isomer through an internal electrostatic stretching force, Biophysical Journal 91 (2006) 3607–3616.
[30] D.R. Latulippe, A.L. Zydney, Radius of gyration of plasmid DNA isoforms from static light scattering, Biotechnology and Bioengineering 107 (2010) 134–142.
[31] M. Hammermann, C. Steinmaier, H. Merlitz, U. Kapp, W. Waldeck, G. Chirico, J. Langowski, Salt effects on the structure and internal dynamics of superhelical DNAs studied by light scattering and Brownian dynamics, Biophysical Journal 73 (1997) 2674–2687.
[32] Y. Lyubchenko, L. Shlyakhtenko, Visualization of supercoiled DNA with atomic force microscopy in situ, Proceedings of the National Academy of Sciences of the United States of America 94 (2007) 496–501.
[33] T.C. Boles, J. White, H.N.R. Cozzarelli, Structure of plectonemically supercoiled DNA, Journal of Molecular Biology 213 (1990) 931–951.
[34] F. Sousa, S. Freitas, A.R. Azzoni, D.M.F. Prazeres, J. Queiroz, Selective purification of supercoiled plasmid DNA from clarified cell lysates with a single histidine–agarose chromatography step, Biotechnology and Applied Biochemistry 45 (2006) 131–140.
[35] K.J. Kim, P.V. Stevens, Hydraulic and surface characteristics of membranes with parallel cylindrical pores, Journal of Membrane Science 123 (1997) 303–314.
[36] W.S. Opong, A.L. Zydney, Diffusive and convective protein transport through asymmetric membranes, AIChE Journal 37 (1991) 1497–1510.
[37] W.R. Bowen, A.W. Mohammad, N. Hilal, Characterization of nanofiltration membranes for predictive purposes—use of salts, uncharged solutes and atomic force microscopy, Journal of Membrane Science 126 (1997) 91–105.
[38] D.M.F. Prazeres, Prediction of diffusion coefficients of plasmids, Biotechnology and Bioengineering 99 (2008) 1040–1044.